Polymer 69 (2015) 283–292

Contents lists available at ScienceDirect

Polymer

journal homepage: www.elsevier.com/locate/polymer

Optimisation of epoxy blends for use in extrinsic self-healing fibre-reinforced composites

Daniel T. Everitt [a], Rafael Luterbacher [a], Tim S. Coope [a], Richard S. Trask [a], Duncan F. Wass [b], Ian P. Bond [a, *]

[a] Advanced Composites Centre for Innovation and Science, Department of Aerospace Engineering, University of Bristol, Queen's Building, BS8 1TR, United Kingdom
[b] School of Chemistry, University of Bristol, BS8 1TH, United Kingdom

ARTICLE INFO

Article history:
Received 18 December 2014
Received in revised form
25 February 2015
Accepted 26 February 2015
Available online 7 March 2015

Keywords:
Self-healing materials
Toughened epoxies
Composite materials

ABSTRACT

A range of epoxy blends were investigated to determine their mechanical properties and suitability for use as healing agents for the repair of fibre-reinforced polymer (FRP) composites. Key requirements for an effective healing agent are low viscosity, and good mechanical performance. A base epoxy resin was selected and blended with a variety of diluents and a toughening agent, and the physical and mechanical properties of the resulting polymers were investigated. Single lap shear strengths of up to 139% of the base epoxy values were demonstrated, while double cantilever beam testing showed specimens healed with optimised epoxy blends can provide recoveries in fracture toughness of up to 269%, compared to 56% in specimens healed with the base epoxy resin. Cross-ply FRP laminate tensile specimens were used to highlight the potential to recover stiffness decay caused by intraply cracking. Following infusion of the damage via embedded vascules, the toughened epoxies were capable of providing complete recovery of stiffness.

1. Introduction

Self-healing materials have attracted a considerable amount of research interest in recent years, with significant advances in both intrinsic and extrinsic healing methods [1,2]. Healing mechanisms have been developed for a range of host materials, ranging from polymers [3–5] to cementitious materials [6]. Another area of particular interest has been fibre-reinforced polymer (FRP) composite materials, which are used widely in the aerospace and renewable energy industries. Efforts to construct civil aircraft from these lightweight materials are expanding in order to reduce fuel consumption and CO_2 emissions. Due to the complex damage and failure mechanisms seen in FRPs [7], composite aircraft are currently built with a high level of redundancy, reducing potential structural mass savings. In the long-term, a shift from the current philosophy of 'no damage growth' to a more advanced damage-tolerant design approach is envisioned. The realisation of smarter materials and structures will further this aim, with self-sensing and self-repairing technologies being key areas of research.

Within the research developments of self-healing FRPs, the vascular network [8–14] approach has largely dominated in recent years. The laminar nature of composites makes the manufacture of 1- and 2-dimensional networks relatively simple [12,15]; 3-D networks have also been demonstrated [11,16]. Healing has been achieved by both the injection of premixed healing agents [17] and post-damage mixing of a 2-part system [18,19].

Despite a body of research into the nature of vascules themselves, their arrangement within FRPs and demonstration of their healing performance, relatively little focus has been given to the nature of the healing agent that is deployed via the network. Dicyclopentadiene (DCPD), in combination with first generation Grubbs' catalyst, was the first extrinsic healing agent used in FRPs [20] and has been successfully proven in a variety of configurations [21–23]. However, the high price of the Ruthenium catalyst and its sensitivity to air and moisture prohibits use in larger scale applications. Cyanoacrylates [24] and polyesters [25] have recently been considered as healing agents in FRPs, however the majority of healing agents in use up to date have been epoxy based systems [9,15,26–32]. Low viscosity is a key requirement for the healing

* Corresponding author.
E-mail addresses: daniel.everitt@bristol.ac.uk (D.T. Everitt), i.p.bond@bristol.ac.uk (I.P. Bond).

http://dx.doi.org/10.1016/j.polymer.2015.02.047

agents in order to achieve effective infusion of damage. A variety of non-reactive diluents such as ethyl phenylacetate (EPA) [26] and acetone [9], as well as reactive diluents such as alkyl glycidyl ether [27] have been used. In some cases commercially available low-viscosity epoxies such as those used for resin infusion [15,28] or potting compounds [29,30] have also been employed. However, these epoxies are often unsuitable as structural materials or possess other characteristics e.g. prolonged cure cycle, which make them sub-optimal for use as healing agents in high performance composite structures.

Herein we aim to demonstrate an epoxy resin optimised for use as a healing agent for infusion of damage within FRPs via a vascular network. The key requirements were identified as: (1) low viscosity, to enable infusion into low-volume damage; (2) good compatibility with the host matrix, to ensure effective re-bonding of fracture surfaces; and (3) high toughness, to prevent further damage in the healed region. Typical commercial low-viscosity, and often low molecular weight, epoxies lack toughness in particular, which is addressed here through the precipitation of toughening particles into the resin and the use of reactive diluents. This research, therefore, builds upon the existing body of research into toughened epoxies by considering a DGEBA based resin system with a carboxyl-terminated butadiene acrylonitrile (CTBN) adduct [33–35].

A baseline diglycidyl ether bisphenol A (DGEBA) based resin system, Epon 828 (Polysciences, Inc.), was investigated in combination with a range of reactive diluents and a toughening agent, HyPox RA840 (Emerald). The studied reactive diluents were D.E.R.736 from Dow Chemicals (a mixture of epichlorohydrin and propylene glycol, (further referred to as **A**)) and poly(propylene glycol)diglycidyl ether (further referred to as **B**). A summary of resin constituents is provided in Fig. 1. Epon 828 was selected as a baseline resin due to the absence of additives or diluents of unknown concentration, as found in many commercial resin systems, along with its fundamental similarity to a number of commercial prepreg resin systems [36]. HyPox RA840 (further referred to as RA840) is a DGEBA based resin system with a carboxyl-terminated butadiene acrylonitrile (CTBN) adduct on 19% of epoxy monomers. Upon reaction with the hardener (DETA), CTBN is displaced from the epoxy monomer, which precipitates particles into the resulting polymer and contributes to increasing the toughness of the cured self-healing polymer.

Cured polymer blends were assessed for their degree of cure, glass transition temperature (T_g) and lap shear strength, as well as their capacity to recover strength and Mode I fracture toughness in FRP double cantilever beam (DCB) specimens.

In order to demonstrate the healing capabilities that are possible through optimisation of the healing agent, mitigation of transverse damage was carried out with some resin blends within cross-ply FRP laminate tensile specimens. FRPs can fail due to a variety of causes, and certain failure modes can be distinctive such as fibre failure, interlaminar failure (delaminations) or intralaminar failure (fibre debonding or matrix cracking) [37]. Self-healing within FRPs is currently limited to repairing the polymeric matrix material and the main focus has been on the interlaminar failure due to the ease by which this larger scale damage can be infused [26]. However, matrix cracking is both the initiating point for delaminations and also the mechanism by which delaminations migrate into adjacent ply interfaces.

In order to determine the effectiveness of the new healing resins developed herein, FRP specimens were designed to encourage the controlled formation of damage which can then be repaired by infusion of the resin blends. The first damage mode for cross-ply laminates [38] (e.g. a laminate with a lay-up of $[0^\circ_n/90^\circ_m]_s$) is matrix cracking. With increasing load the density of matrix cracking in the 90° layer increases, until a load is reached that results in failure of the 0° fibres. Damage to the transverse lamina results in a global stiffness reduction, which can be mitigated by infusion and curing of a healing agent. While manual injection of the healing resin is carried out here, the vasculature could be employed as part of an autonomous healing network. The development of such a system was outside the scope of this work, however a system similar to the one described by Norris et al. [39] or Minakuchi et al. [40] could be easily implemented. In addition, future work is planned to use the developed healing agent in conjunction with catalysts such as scandium triflate [4]. As the healing agents are DGEBA based, a similar encapsulation strategy as described by Ref. [5] could be followed, enabling the use as an autonomous self-healing solution.

2. Experimental

2.1. Materials

Poly(propylene glycol) diglycidyl ether, D.E.R 736 (Dow Chemicals) and diethylenetriamine (DETA) were purchased from Sigma–Aldrich UK. Epon 828 was purchased from Polysciences, Inc.

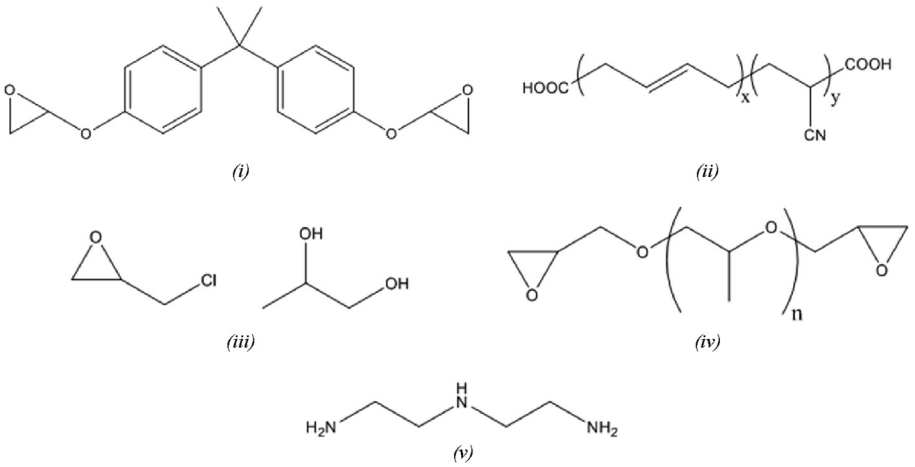

Fig. 1. Chemical structures of (*i*) diglycidyl ether bisphenol A (DGEBA), (*ii*) carboxyl-terminated butadiene acrylonitrile (CTBN), (*iii*) epichlorohydrin, propylene glycol (D.E.R 736) (**A**), (*iv*) poly(propylene glycol) diglycidyl ether (**B**), (*v*) diethylenetriamine (DETA).

Europe. Hypox RA840 (Emerald) was provided by Hubron Speciality Ltd. IM7/8552 carbon/epoxy and 913 E-glass/epoxy pre-impregnated tape were purchased from Hexcel.

2.2. Differential scanning calorimetry

Resin blends were thoroughly mixed and approximately 10 mg was quickly transferred to Tzero aluminium hermetic pans. A TA Q200 DSC was used to study cure behaviour via modulated dynamic scans. A heating rate of 10 °C min^{-1} and a temperature range of 0 °C–250 °C was used. Nitrogen purge gas flow rate = 50 ml min^{-1}. T_g values were obtained over a temperature range of −30 °C–200 °C with a heating rate of 3 °C min^{-1}.

2.3. Viscometry

All viscosity readings were taken on a Brookfield DV-E viscometer at 24 ± 1 °C. Blends were mixed thoroughly and readings were taken before addition of the hardener until stable, with final reported readings taken immediately after adding the hardener component.

2.4. Tensile specimen manufacture & testing

Type IV tensile specimens were prepared according to ASTM D 638 [41]. Additive layer manufacturing was used to create a positive mould from which silicone moulds were cast. Resin blends were mixed, degassed and poured into the moulds before an aluminium top plate was applied to ensure a flat surface. Specimens were cured for 1 h at 45 °C and left for a minimum of 5 days at ambient temperature before testing.

Testing was conducted on a Shimadzu AGS-X universal test machine fitted with a calibrated 10 kN load cell at a rate of 20 mm min^{-1}.

2.5. Single lap shear specimen manufacture & testing

Carbon fibre/epoxy unidirectional (UD) prepreg (IM7 8552, Hexcel, UK) panels were manufacture by hand layup. A cure cycle of 60 min at 110 °C followed by 120 min at 180 °C was carried out, both under 700 kPa pressure, as per the manufacturer's specifications. Substrate panels were cut to size (75 mm × 135 mm × 2.8 mm, 20 plies) on a diamond coated saw. End tabs of the same material were bonded using Elantech epoxy adhesive.

Bonding surfaces of each substrate were grit blasted and cleaned prior to addition of the investigated healing agent. Two substrate panels were then clamped and cured before cutting to final size (75 mm × 25 mm × 2.8 mm). Specimens were found by microscopy to have a bond thickness of approximately 50 μm. A schematic of the specimen geometry can be seen in Fig. 2.

Testing was carried out with reference to ASTM D 5868 [42] and AITM 1-0019 [43] on a Schenck Hydropuls PSA universal test machine fitted with a calibrated 75 kN load cell at a rate of 2 mm min^{-1}. A lower test rate as indicated by the ASTM standard was selected in order to compare to former tests. The initial grip to grip separation during testing was 75 mm.

Lap shear strength (MPa) was calculated by dividing the failure load by the bonded area, nominally 25 mm × 25 mm.

$$\sigma_{SLS} = \frac{P_{max}}{w\ l} \quad (1)$$

In which P_{max}, w and l refer respectively to the failure load (N), width (mm) and length (mm) of the bond area.

2.6. Mode I specimen manufacture, healing & testing

Carbon fibre/epoxy unidirectional (UD) prepreg (IM7/8552, Hexcel, UK) panels (600 mm × 180 mm × 3.4 mm, 24 plies) featuring a 15 μm release film insert were manufactured by hand lay-up so as to result in an initial delamination length (a_0) of 50 mm. A cure cycle of 60 min at 110 °C followed by 120 min at 180 °C, both under 700 kPa pressure in an autoclave, was carried out, as per the manufacturer's specifications. Specimens were cut to size (160 mm × 20 mm × 3.4 mm) on a diamond coated saw and piano hinges were bonded onto grit blasted surfaces using an Elantech epoxy cured at ambient temperature overnight as preparation for testing. A schematic is provided in Fig. 3.

Testing was carried out according to ASTM D 5528 [44] on a Shimadzu AGS-X universal test machine fitted with a calibrated 1 kN load cell at a rate of 5 mm min^{-1}. Cracks were propagated for approximately 50 mm. A Labview™ script was used to acquire the delamination length via high resolution images (to an accuracy greater than ±0.5 mm), displacement and load data.

Specimens were healed after the initial fracture via injection of the healing resin onto the fracture surface. Specimens were then taped closed and cured for 1 h at 45 °C and left for a minimum of 5 days at ambient temperature prior to repeat testing.

Load P (in N), displacement δ (in mm), crack length a (in mm), specimen width b (in mm) and specimen thickness t (in mm) were used to determine Mode I strain energy release rate G_{IC} (in J m^{-2}) via the modified beam theory (MBT) method [44]. A compliance calibration factor (Δ) is used to correct for any rotation at the crack front, which causes effective elongation of the delamination (a + |Δ|). Δ is determined from the gradient (m) and intercept (c) of a plot of the cube root of compliance ($C^{1/3}$) against crack length:

$$\Delta = \left|\frac{-c}{m}\right| \quad (2)$$

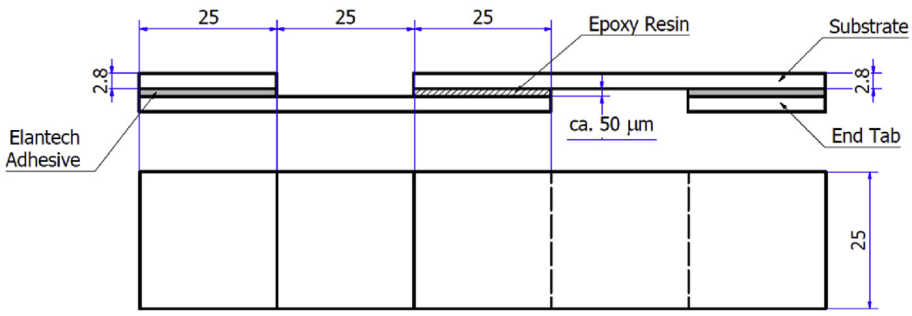

Fig. 2. Schematic of the SLS specimens. Dimensions are given in mm.

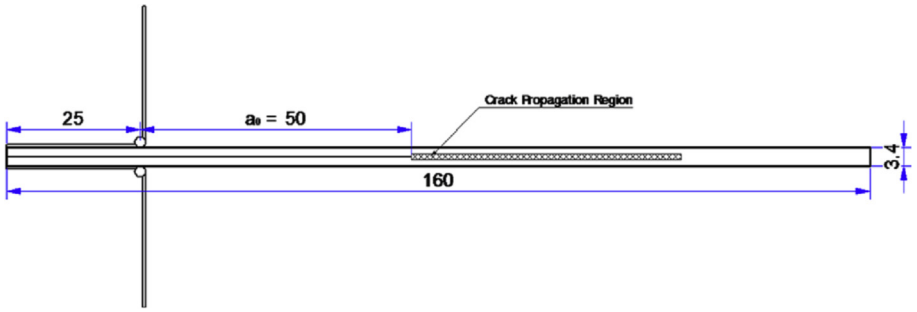

Fig. 3. Schematic depicting the hinged DCB specimens. The PTFE insert creates a precrack length (a_0) of 50 mm from the point of loading. Dimensions are given in mm.

$$G_{IC} = \frac{3P\delta}{2b(a + |\Delta|)} \tag{3}$$

Healing efficiencies (ζ) are given as percentages in terms of fracture toughness (G_{IC}) and peak load (P).

$$\zeta_{G_{IC}} = \frac{G_{IC_{Healed}}}{G_{IC_{Pristine}}} \tag{4}$$

$$\zeta_{P} = \frac{P_{Healed}}{P_{Pristine}} \tag{5}$$

2.7. Cross-ply manufacture, healing & testing

For ease of damage identification via back light illumination, glass fibre-reinforced polymer composites were selected. Panels (220 mm × 150 mm) of unidirectional 913/E-Glass (Hexcel, UK) were manufactured by hand lay-up. The manufacturer's recommended cure cycle of 125 °C for 1 h and 700 kPa was followed. Self-healing specimens had a PTFE coated NiCr wire (The Scientific Wire Company) incorporated in a cut out of the $90_2/0_2$ plies (refer to Fig. 4) in order to manufacture the vascular network (*Procedure B* as described by Norris et al. [10]). This interface was selected in order to assure that the transverse damage occurring in the 90 ° plies will intersect with perpendicular with the vascule. After cure, the wire was removed and end tabs were bonded using Elantech epoxy adhesive. Specimens were then cut to size on a diamond saw (200 mm × 20 mm × 2.2 mm) (see Fig. 5).

Cross-ply laminates were tested with reference to ASTM D3039 [45] at a rate of 2 mm min^1 on a Schenck Hydropuls PSA universal testing machine equipped with a calibrated 75 kN load cell. Specimens for healing were loaded to 15 kN (ca. 70% of the failure load) and unloaded. Strain was measured on the central 50 mm of the specimen using a video extensometer (Imetrum). The modulus was determined on the loading ($E_{pristine}$) and unloading ($E_{damaged}$) parts, between 20 MPa and 100 MPa.

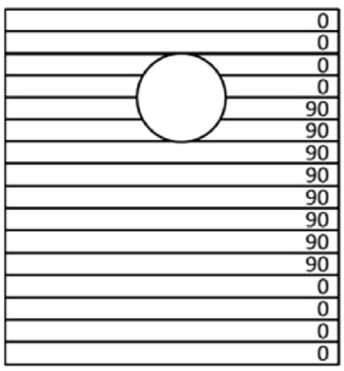

Fig. 4. Layup of cross-ply laminates. A 0.5 mm diameter vascule is placed such that it will provide connectivity with any transverse damage formed in the 90° plies.

Prior to infusion of the healing agent, the edges of the specimens were sealed. Healing agent was delivered to the vascular network with a syringe pump (Nexus) for 10 min at a flow rate of 0.2 ml min^{-1}, and the specimens were cured and retested. The modulus was once again determined upon loading (E_{healed}).

The healing performance was determined, as follows, in accordance with Blaiszik et al. [1]:

$$\zeta = \frac{E_{healed} - E_{damaged}}{E_{pristine} - E_{damaged}} \tag{6}$$

3. Results & discussion

3.1. Polymer blends

Diethylenetriamine (DETA) was used to cross-link all blends discussed herein. Hardener concentration was determined for each blend based on epoxide-equivalent weight (EEW) calculations [46]. Concentrations of different epoxies and hardener used in each blend are shown in Table 1. The effect of non-stoichiometric mixing on resin properties will be investigated in future work.

$$\text{Amine H eq. wt.} = \frac{M_w \text{ of amine}}{\#\text{ active hydrogens}} \tag{7}$$

$$\text{pph of amine} = \frac{\text{Amine H eq. wt.} \times 100}{\text{Blend EEW}} \tag{8}$$

EEWs of resin blends were calculated as so:

$$\text{Blend EEW} = \frac{\text{Total wt.}}{\frac{wt._a}{EEW_a} + \frac{wt._b}{EEW_b} + \frac{wt._c}{EEW_c}} \tag{9}$$

where a range of EEWs was provided for a given healing agent, the mean value was used.

Given that low viscosity was identified as a key characteristic of any target healing resin, and the high viscosity of RA840 (440 000 cP), a maximum of 20 wt% RA840 was used. Tripathi et al. [33] found that 20 wt% of CTBN within a DGEBA-based resin was optimum for increasing toughness; thus, a similar value was targeted for the blends presented herein. Rubber particles precipitated upon curing of the Epon 828 + RA840 blend by DETA can be seen in Fig. 6. Typical particles are approximately 50 μm in diameter.

3.2. Thermal analysis

Epon 828 has a recommended cure cycle of 7 days at ambient temperature. Here, a cycle of 1 h at 45 °C followed by a minimum of 5 days at ambient temperature was used for all blends.

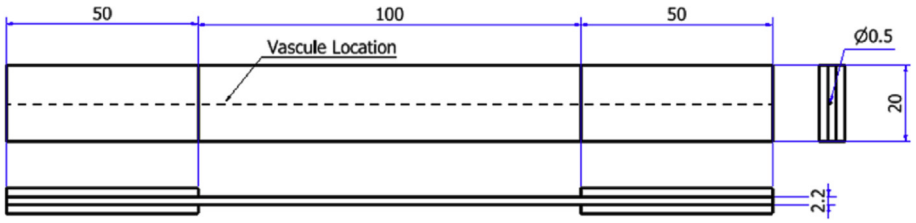

Fig. 5. Cross-ply laminate geometry.

Table 1
Summary of properties of each epoxy blend.

Blend ID	Epon 828 (wt %)	HyPox RA840 (wt %)	Diluent (wt %)		Hardener concentration (pph)	T_g (°C)	Viscosity (cP)[a]	Tensile Strength[b]/MPa	SLS[c]/MPa
			A	B					
Epon	100	0	0	0	12	115	1900	73 ± 11	12 ± 0.4
EponRA840	80	20	0	0	10.8	105	2210	52 ± 4	21 ± 4
20A	60	20	20	0	10.6	82	1203	52 ± 8	18 ± 3
30A	50	20	30	0	10.5	48	680	62 ± 3	25 ± 1
40A	40	20	40	0	10.4	45	568	39 ± 6	29 ± 1
50A	30	20	50	0	10.2	9	357	14 ± 1	18 ± 2
20B	60	20	0	20	9.5	79	1416	32 ± 2	24 ± 28
30B	50	20	0	30	8.8	47	750	46 ± 8	28 ± 1
40B	40	20	0	40	8.1	42	702	48 ± 1	20 ± 1
50B	30	20	0	50	7.4	34	358	4 ± 0.3	8 ± 1

[a] All viscosity readings were carried out immediately after addition of the hardener at 24 ± 1 °C.
[b] ASTM D 638, minimum of 4 specimens.
[c] ASTM D 5868, minimum of 3 specimens.

Optimisation of the cure cycle was outside the scope of this work, however, preliminary analyses indicated that significantly faster curing is possible at higher temperatures. It is thought that higher cure temperature will also result in higher T_g values. Further investigation of alternative cure cycles will be carried out in the future. Modulated DSC analysis was used to confirm complete curing of all blends; plots are shown in Fig. 7.

The influence of diluent concentration on glass transition temperature (T_g) was also investigated by DSC. T_g data are summarised in Table 1. T_g drops rapidly as diluent concentration increases. This observation is consistent with mechanical testing data showing increasing ductility of the resulting polymers. In the case of **A** the increased ductility is attributed to the reduction in chain length caused by the mono-functional epoxy, epichlorohydrin, and presence of the non-reactive diluent, propylene glycol [47,48]. Diluent **B**, poly(propylene glycol) diglycidyl ether, is a bifunctional epoxy monomer which, due to its length and lack of bulky groups, increases polymer chain flexibility.

3.3. Mechanical testing

3.3.1. Lap shear

Lap shear testing was carried out with reference to ASTM 5868 [42] and AITM 1-0019 [43]. Lap shear testing was selected as an efficient method to screen a high number of candidate polymer blends for lap shear strength and to investigate a mixed mode loading condition on the adhesive layer [49]. This loading

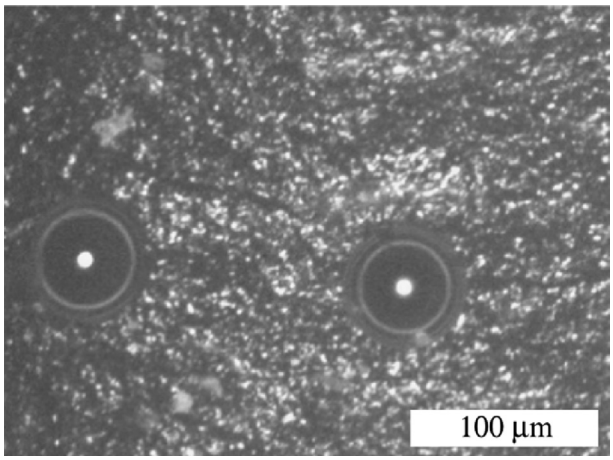

Fig. 6. Particles of CTBN precipitated by 20 wt% HyPox RA840 within Epon 828 epoxy resin hardened with DETA.

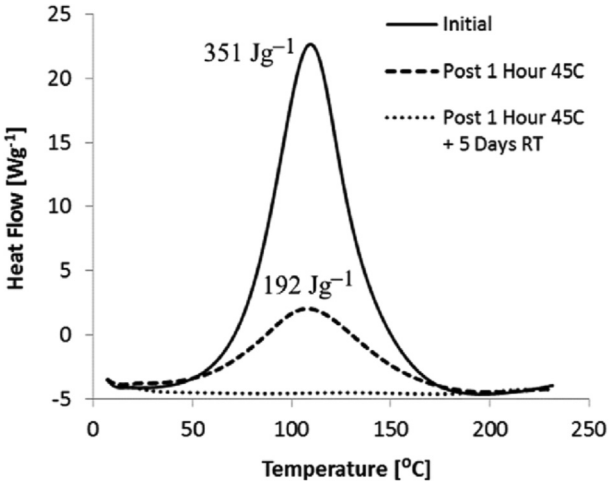

Fig. 7. Overlaid MDSC traces showing completion of resin cure after 1 h at 45 °C and 5 days at room temperature for Epon 828/RA840 50B. Equivalent plots were obtained for all blends.

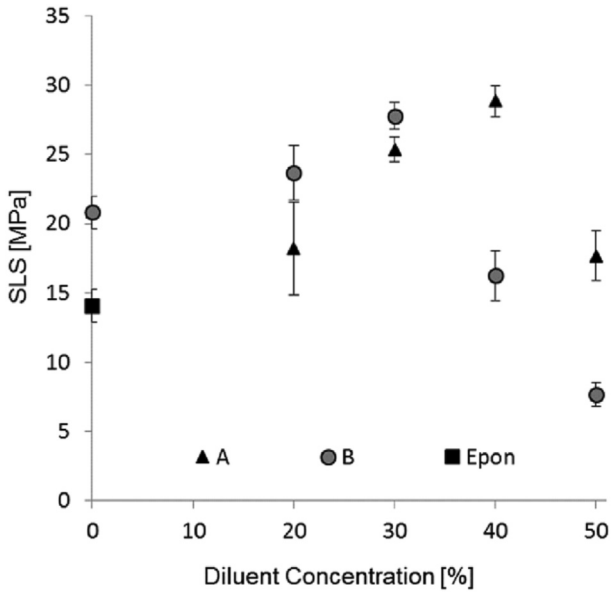

Fig. 8. Influence of varying concentration of reactive diluents on single lap shear strength of specimens bonded with RA840 toughened Epon 828. Baseline Epon 828 performance is included for comparison.

condition, therefore, corresponds to a more realistic damage propagation scenario in FRP structures.

Variation in single lap shear (SLS) strength as a function of diluent concentration can be seen in Fig. 8 and Table 1. Introducing 20 wt% of the toughening agent RA840 showed an increase in SLS strength to 148% of baseline Epon 828 values. SLS strength peaks at 29 MPa with 40 wt% of diluent **A** and at 28 MPa with 30 wt % of diluent **B**, within Epon 828/RA840 (20 wt%). SLS decreases rapidly after these peaks.

3.3.2. Mode I fracture mechanics evaluation

Determination of self-healing performance of epoxy blends was carried out via double cantilever beam (DCB) testing according to ASTM Standard D5528 [44]. Specimens were fractured, unloaded, healed and retested to failure.

Table 2 provides a summary of pristine and healed DCB performance, along with healing efficiency values, which are also summarised in Fig. 9. Specimens healed with the baseline Epon 828 achieved a mean peak load healing efficiency (ζ_P) of 84%, however, the fracture toughness of the healed specimens was poor, just 56% of the baseline material. Upon addition of 20 wt% of RA840 (Epon828 + RA840) these values improved to $\zeta_P = 169\%$, $\zeta_{GIC} = 87\%$ respectively, demonstrating the effectiveness of the additive at increasing failure load. However, only a relatively small improvement was seen with fracture toughness; from 56% recovery with Epon 828 to 87% with RA840 toughened Epon 828.

Table 2
Summary of peak load and fracture toughness values obtained from pristine and healed DCB specimens. A minimum of 3 tests were carried out per data point.

Blend ID	Epon 828 (wt%)	HyPox RA840 (wt%)	Diluent (wt%)		Pristine		Healed			
			A	B	Peak load (P)/N	Initial fracture toughness (G_{IC})/Jm^{-2}	Peak load (P)/N	Mean efficiency (ζ_P)	Initial fracture toughness (G_{IC})/Jm^{-2}	Mean efficiency (ζ_{GIC})
Epon	100	0	0	0	42 ± 4	279 ± 21	37 ± 2	88%	158 ± 77	56%
EponRA840	80	20	0	0	44 ± 6	271 ± 35	76 ± 10	169%	235 ± 100	87%
30A	50	20	30	0	43 ± 1	294 ± 37	68 ± 2	159%	764 ± 24	270%
40A	40	20	40	0	43 ± 2	255 ± 4	60 ± 5	141%	680 ± 123	266%
50A	30	20	50	0	38 ± 3	285 ± 23	68 ± 2	180%	701 ± 75	246%
30B	50	20	0	30	40 ± 6	280 ± 63	71 ± 12	177%	762 ± 148	272%
40B	40	20	0	40	40 ± 3	299 ± 42	61 ± 6	152%	592 ± 176	198%
50B	30	20	0	50	43 ± 3	272 ± 5	57 ± 6	131%	552 ± 112	203%

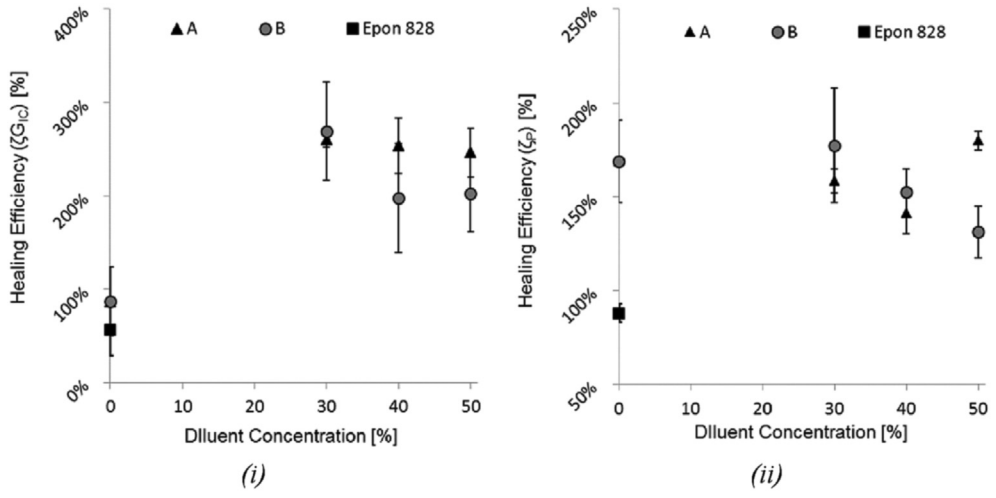

Fig. 9. Influence of concentration of diluents A and B in Epon + RA840 on healing efficiency in terms of *i*) initial fracture toughness (ζ_{GIC}) and *ii*) peak load (ζ_P). Baseline Epon data are also included.

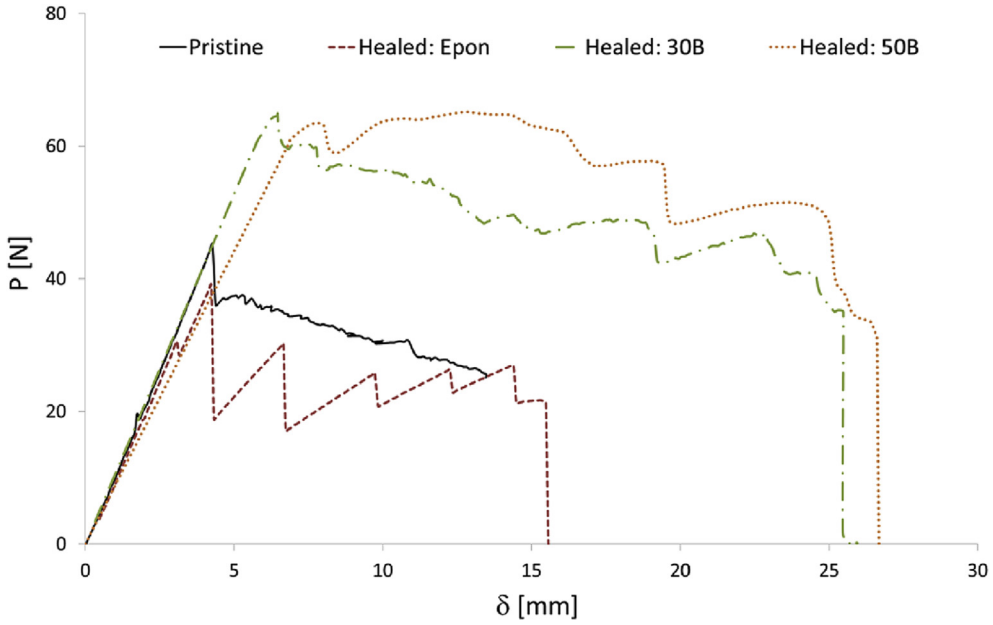

Fig. 10. Representative load displacement plots of pristine IM7 8552 DCBs and specimens healed with Epon 828, RA840 toughened Epon 828 with 30 wt% of reactive diluent B (30B) and RA840 toughened Epon 828 with 50 wt% of reactive diluent B (50B).

Upon addition of reactive diluents **A** or **B** to the Epon828 + RA840 blend, mixed viscosity reduced significantly, as shown in Table 1. This effect was seen to improve lap shear strength up to a critical point (28 MPa) after which resin performance fell rapidly, as shown in Fig. 8. DCB testing allows investigation of the impact of diluents on resin fracture toughness and healing efficiency. Diluent loadings below 30 wt% were not investigated as their viscosities were considered too high (>1200 cP) for successful damage infusion within more realistic composite specimens. The addition of 30 wt% of diluent resulted in a sharp increase in ζ_{GIC}. Further increasing diluent concentration resulted in a reduction to ζ_{GIC} relative to the peak obtained at 30 wt%. In terms of DCB failure load recovery, however, the impact of diluent concentration was shown to be much smaller than in the case of fracture toughness (Fig. 9). Increasing diluent concentration from 0% to 30% does not cause ζ_P to vary significantly from values seen in specimens healed with Epon + RA840. Therefore, it is apparent that the presence of RA840 can significantly increase failure load recovery (from 87% with plain Epon, to 169% when 20 wt% of RA840 is also present), whereas the presence of diluents can significantly increase fracture toughness recovery from below 100% to over 250%.

Representative load–displacement behaviour for specimens healed with Epon 828, 30B and 50B (Table 1) compared with a baseline specimen can be seen in Fig. 10. Here, the brittle nature of specimen failure when healed with the baseline resin (Epon 828) is apparent. In comparison, the addition of 30 wt% of either diluent **A** (30A) or **B** (30B) is seen to significantly increase ductility and lead to stable crack propagation (Fig. 11), with high fracture toughness recoveries of around 250%. At 50 wt% of diluent this ductility remains, but lower healing efficiencies of 200% fracture toughness recovery are obtained (Fig. 12).

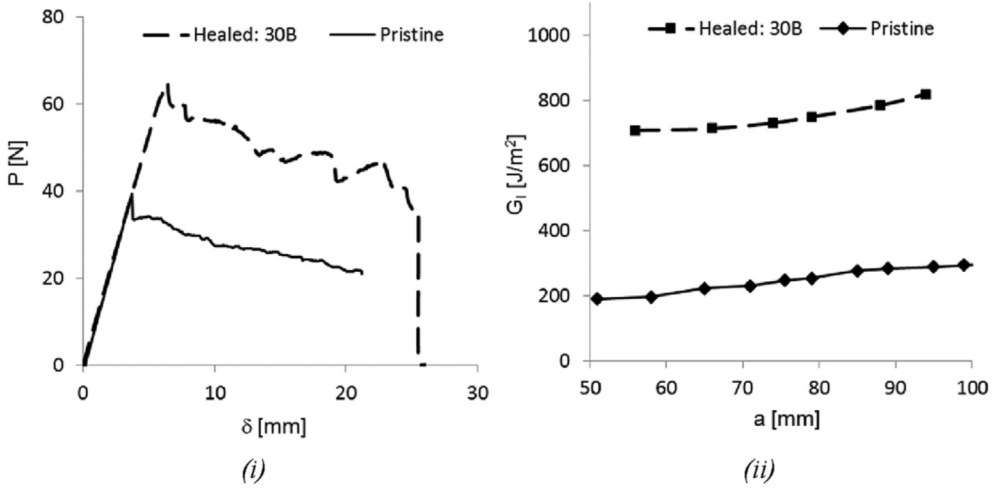

Fig. 11. *i*) Representative load–displacement plots for a DCB specimen before and after healing with 30B. A peak load recovery (ζ_P) of 153% is observed. *ii*) Fracture toughness vs. crack length for the same specimen before and after healing with 30B. A fracture toughness recovery (ζ_{GIC}) of 250% is observed.

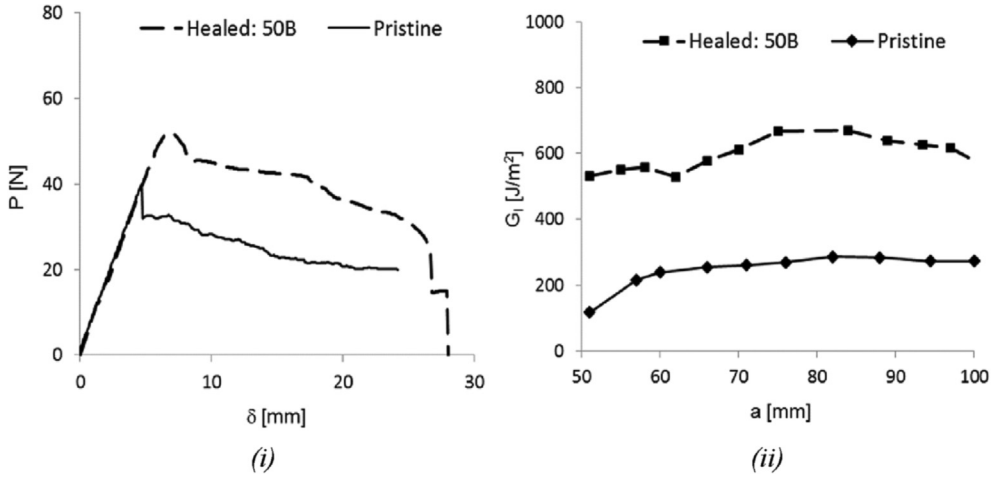

Fig. 12. *i*) Representative load–displacement plots for a DCB specimen before and after healing with 50B. A peak load recovery (ζ_P) of 130% is observed. *ii*) Fracture toughness vs. crack length for the same specimen before and after healing with 50B. A fracture toughness recovery (ζ_{GIC}) of 203% is observed.

4. Repair of transverse damage in cross-ply laminates

Cross-ply laminates vulnerable to the development of transverse matrix cracking were used to further demonstrate the capacity for using the developed epoxy blends for repair of FRPs. Manual infusion of the damage via a vascule was carried out in this case. While outside the scope of this work, integration into an autonomous healing system is feasible. Either using the vascule as a pressure sensor [39] or an additional integrated strain sensor system [40] could trigger the mixing and release of the healing agent

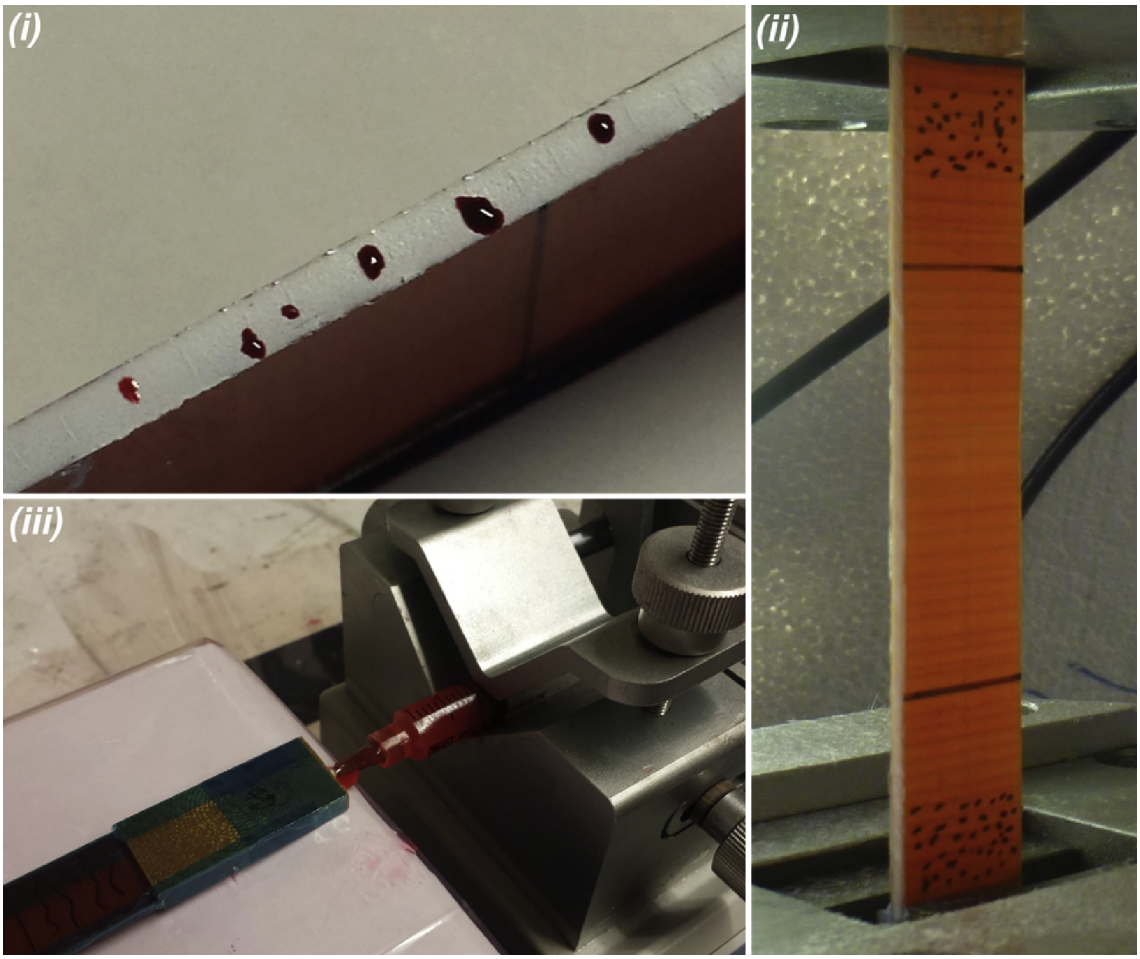

Fig. 13. *i*) Here the injection of dye penetrant (Ardrox 996 PA) through the longitudinal vascule results in 'bleeding' from the side of the specimen (via damage in the 90° plies), demonstrating connectivity between the centrally located vascule and internal damage. *ii*) Transverse matrix damage spanning the test specimen width in a cross-ply laminate, resulting from tensile loading. *iii*) Infusion of healing resin into a damaged cross-ply specimen.

Table 3
Summary of the healing performance. A minimum of 5 tests were carried out per data point.

Blend ID	Epon 828 (wt%)	Hypox RA840 (wt%)	Diluent (wt%)		Healing efficiency (ζ)
			A	B	
40A	40	20	40	0	106% ± 31%
30B	50	20	0	30	114% ± 38%
50B	30	20	0	50	119% ± 30%

into the vascule. Then a heating solution such as an incorporated resistive heating mat could provide a localised healing solution. The infusion of a low viscosity red dye penetrant (Ardrox 996 PA) clearly visualised the connectivity between the vascule and the transverse damage (Fig. 13 i).

Table 3 summarises the healing performance for the cross-ply FRP laminate infusion tests. The resins 40A, 30B and 50B were used to heal damage cross-ply specimens. Full recovery of stiffness was achieved with all resin systems.

Section 2.7 provides details of specimen and test configuration. The development of matrix cracking plays a crucial role in both delamination initiation and migration in FRPs, and is therefore a key target damage state for self-healing solutions. In the case of DCB specimens [10] the vascule is located in the damage plane, thereby ensuring easy wet-out of the fracture surface. However, in the case of the cross ply laminates, the damage intersects the vascule perpendicularly. This intraply damage is much smaller in volume than in the case of delaminations in DCB specimens, therefore, the resin flow into these damage locations is perturbed in comparison to that in DCBs. This limited connectivity between vasculature and damage, combined with trapped air in some locations, gives rise to incomplete infusion during healing, and is responsible for the high standard deviations observed for the achieved healing efficiencies.

The investigated healing agent blends were observed to fully recover stiffness in all cases. Thus, healing agent formulation and selection will be driven more by requirements for failure strength and fracture toughness performance alongside physical and processing characteristics e.g. viscosity, cure kinetics, T_g.

5. Conclusions

It was found that by addition of 20 wt% of HyPox RA840 to Epon 828 epoxy, the precipitation of 50 μm diameter toughening particles significantly improved the tensile strength in single lap shear, and fracture toughness in Mode I double cantilever beam tests. From a constant concentration of 20 wt% HyPox RA840, increasing the concentration of a reactive diluent (Dow Chemicals' D.E.R 736 **(A)** or poly(propylene glycol) diglycidyl ether **(B)**) while reducing the concentration of Epon 828 showed to increase polymer ductility, resulting in an increasingly ductile failure in Mode I (DCB) testing. DCB testing also revealed that the addition of these reactive diluents significantly increased fracture toughness (G_{IC}). It has been demonstrated that the investigated epoxies are highly effective at repairing DCB specimens. Furthermore, the potential for full recovery of stiffness in specimens affected by transverse matrix damage was demonstrated by the infusion of cross-ply FRP laminates with the developed healing agent blends.

Overall, blend 30B (20wt% HyPox RA840, 50wt% Epon 828, 30wt % diluent **B**) was found to offer the best range of physical and mechanical properties; fulfilling the requirement for low viscosity while offering high strength and toughness. Therefore, the investigation and optimisation of this polymer blend has identified the true potential to realising high performance vascularised self-healing FRP composites, via an extrinsic method [39,40].

Acknowledgements

The authors would like to thank the EPSRC (EP/G036772/1) and Fundació Obra Social La Caixa for funding. We would also like to thank Dr Julie Etches for her assistance with DCB data collection, Ian Chorley and Glenn Wallington for their assistance in the laboratory and Martin F. Cicognani from Hubron Speciality for his support and for providing the HyPox RA840.

References

[1] Blaiszik BJ, Kramer SLB, Olugebefola SC, Moore JS, Sottos NR, White SR. Self-healing polymers and composites. Annu Rev Mater Res 2010;40:179–211. http://dx.doi.org/10.1146/annurev-matsci-070909-104532.
[2] Yuan YC, Yin T, Rong MZ, Zhang MQ. Self healing in polymers and polymer composites. Concepts, realization and outlook: a review. eXPRESS Polym Lett 2008;2:238–50. http://dx.doi.org/10.3144/expresspolymlett.2008.29.
[3] Wu DY, Meure S, Solomon D. Self-healing polymeric materials: a review of recent developments. Prog Polym Sci 2008;33:479–522. http://dx.doi.org/10.1016/j.progpolymsci.2008.02.001.
[4] Coope TS, Mayer UFJ, Wass DF, Trask RS, Bond IP. Self-healing of an epoxy resin using Scandium(III) triflate as a catalytic curing agent. Adv Funct Mater 2011;21:4624–31. http://dx.doi.org/10.1002/adfm.201101660.
[5] White SR, Sottos NR, Geubelle PH, Moore JS, Kessler MR, Sriram SR, et al. Autonomic healing of polymer composites. Nature 2001;409:794–7. http://dx.doi.org/10.1038/35057232.
[6] Wu M, Johannesson B, Geiker M. A review: self-healing in cementitious materials and engineered cementitious composite as a self-healing material. Constr Build Mater 2012;28:571–83. http://dx.doi.org/10.1016/j.conbuildmat.2011.08.086.
[7] Greenhalgh ES. Failure analysis and fractography of polymer composites. Woodhead Publishing; 2009.
[8] Dry C. Procedures developed for self-repair of polymer matrix composite materials. Compos Struct 1996;35:263–9. http://dx.doi.org/10.1016/0263-8223(96)00033-5.
[9] Pang JWC, Bond IP. "Bleeding composites"—damage detection and self-repair using a biomimetic approach. Compos Part A Appl Sci Manuf 2005;36:183–8. http://dx.doi.org/10.1016/j.compositesa.2004.06.016.
[10] Norris CJ, Bond IP, Trask RS. Interactions between propagating cracks and bioinspired self-healing vascules embedded in glass fibre reinforced composites. Compos Sci Technol 2011;71:847–53. http://dx.doi.org/10.1016/j.compscitech.2011.01.027.
[11] Toohey KS, Sottos NR, Lewis JA, Moore JS, White SR. Self-healing materials with microvascular networks. Nat Mater 2007;6:581–5. http://dx.doi.org/10.1038/nmat1934.
[12] Trask RS, Bond IP. Biomimetic self-healing of advanced composite structures using hollow glass fibres. Smart Mater Struct 2006;15:704–10. http://dx.doi.org/10.1088/0964-1726/15/3/005.
[13] Williams HR, Trask RS, Weaver PM, Bond IP. Minimum mass vascular networks in multifunctional materials. J R Soc Interface 2008;5:55–65. http://dx.doi.org/10.1098/rsif.2007.1022.
[14] Bleay SM, Loader CB, Hawyes VJ, Humberstone L, Curtis PT. A smart repair system for polymer matrix composites. Compos Part A Appl Sci Manuf 2001;32:1767–76. http://dx.doi.org/10.1016/S1359-835X(01)00020-3.
[15] Williams G, Trask RS, Bond IP. A self-healing carbon fibre reinforced polymer for aerospace applications. Compos Part A Appl Sci Manuf 2007;38:1525–32. http://dx.doi.org/10.1016/j.compositesa.2007.01.013.
[16] Hansen CJ, Wu W, Toohey KS, Sottos NR, White SR, Lewis JA. Self-healing materials with interpenetrating microvascular networks. Adv Mater 2009;21:4143–7. http://dx.doi.org/10.1002/adma.200900588.
[17] Coope TS, Wass DF, Trask RS, Bond IP. Metal triflates as catalytic curing agents in self-healing fibre reinforced polymer composite materials. Macromol Mater Eng February 2014;299(2):208–18. http://dx.doi.org/10.1002/mame.201300026.
[18] Williams HR, Trask RS, Bond IP. Self-healing sandwich panels: restoration of compressive strength after impact. Compos Sci Technol 2008;68:3171–7. http://dx.doi.org/10.1016/j.compscitech.2008.07.016.
[19] Hamilton AR, Sottos NR, White SR. Self-healing of internal damage in synthetic vascular materials. Adv Mater Deerf 2010;22:5159–63. http://dx.doi.org/10.1002/adma.201002561.
[20] Kessler M, White S. Self-activated healing of delamination damage in woven composites. Compos Part A Appl Sci Manuf 2001;32:683–99. http://dx.doi.org/10.1016/S1359-835X(00)00149-4.
[21] Sanada K, Yasuda I, Shindo Y. Transverse tensile strength of unidirectional fibre-reinforced polymers and self-healing of interfacial debonding. Plast Rubber Compos 2006:67–72.
[22] Kessler M, Sottos N, White S. Self-healing structural composite materials. Compos Part A: Appl Sci Manuf 2003;34:743–53. http://dx.doi.org/10.1016/S1359-835X(03)00138-6.
[23] Patel AJ, Sottos NR, Wetzel ED, White SR. Autonomic healing of low-velocity impact damage in fiber-reinforced composites. Compos Part A Appl Sci Manuf 2010;41:360–8. http://dx.doi.org/10.1016/j.compositesa.2009.11.002.

[24] Fifo O, Ryan K, Basu B. Glass fibre polyester composite with in vivo vascular channel for use in self-healing. Smart Mater Struct 2014;23:095017. http://dx.doi.org/10.1088/0964-1726/23/9/095017.
[25] Zainuddin S, Arefin T, Fahim a, Hosur MV, Tyson JD, Kumar A, et al. Recovery and improvement in low-velocity impact properties of e-glass/epoxy composites through novel self-healing technique. Compos Struct 2014;108:277–86. http://dx.doi.org/10.1016/j.compstruct.2013.09.023.
[26] Coope TS, Wass DF, Trask RS, Bond IP. Repeated self-healing of microvascular carbon fibre reinforced polymer composites. Smart Mater Struct 2014;23:115002. http://dx.doi.org/10.1088/0964-1726/23/11/115002.
[27] Patrick JF, Hart KR, Krull BP, Diesendruck CE, Moore JS, White SR, et al. Continuous self-healing life cycle in vascularized structural composites. Adv Mater 2014;26:4302–8. http://dx.doi.org/10.1002/adma.201400248.
[28] Williams HR, Trask RS, Bond IP. Self-healing composite sandwich structures. Smart Mater Struct 2007;16:1198–207. http://dx.doi.org/10.1088/0964-1726/16/4/031.
[29] Trask RS, Norris CJ, Bond IP. Stimuli-triggered self-healing functionality in advanced fibre-reinforced composites. J Intell Mater Syst Struct 2013;25:87–97. http://dx.doi.org/10.1177/1045389X13505006.
[30] Norris CJ, Bond IP, Trask RS. Healing of low-velocity impact damage in vascularised composites. Compos Part A Appl Sci Manuf 2013;44:78–85. http://dx.doi.org/10.1016/j.compositesa.2012.08.022.
[31] Yin T, Zhou L, Rong MZ, Zhang MQ. Self-healing woven glass fabric/epoxy composites with the healant consisting of micro-encapsulated epoxy and latent curing agent. Smart Mater Struct 2008;17:015019. http://dx.doi.org/10.1088/0964-1726/17/01/015019.
[32] Yin T, Rong MZ, Zhang MQ, Zhao JQ. Durability of self-healing woven glass fabric/epoxy composites. Smart Mater Struct 2009;18:074001. http://dx.doi.org/10.1088/0964-1726/18/7/074001.
[33] Tripathi G, Srivastava D. Effect of carboxyl-terminated poly(butadiene-co-acrylonitrile) (CTBN) concentration on thermal and mechanical properties of binary blends of diglycidyl ether of bisphenol-A (DGEBA) epoxy resin. Mater Sci Eng A 2007;443:262–9. http://dx.doi.org/10.1016/j.msea.2006.09.031.
[34] Thomas R, Yumei D, Yuelong H, Le Y, Moldenaers P, Weimin Y, et al. Miscibility, morphology, thermal, and mechanical properties of a DGEBA based epoxy resin toughened with a liquid rubber. Polymer 2008;49:278–94. http://dx.doi.org/10.1016/j.polymer.2007.11.030.
[35] Bagheri R, Marouf BT, Pearson RA. Rubber-toughened epoxies: a critical review. Polym Rev 2009;49:201–25. http://dx.doi.org/10.1080/15583720903048227.
[36] Wang Q, Storm BK, Houmøller LP, Vej NB. Study of the isothermal curing of an epoxy prepreg by near-infrared spectroscopy. J Appl Polym Sci 2003;87:2295–305.
[37] Cantwell WJ, Morton J. The significance of damage and defects and their detection in composite materials: a review. J Strain Anal Eng Des 1992;27:29–42. http://dx.doi.org/10.1243/03093247V271029.
[38] Lundmark P, Varna J. Damage evolution and characterisation of crack types in CF/EP laminates loaded at low temperatures. Eng Fract Mech 2008;75:2631–41. http://dx.doi.org/10.1016/j.engfracmech.2007.03.004.
[39] Norris CJ, White JAP, McCombe G, Chatterjee P, Bond IP, Trask RS. Autonomous stimulus triggered self-healing in smart structural composites. Smart Mater Struct 2012;21:094027. http://dx.doi.org/10.1088/0964-1726/21/9/094027.
[40] Minakuchi S, Sun D, Takeda N. Hierarchical system for autonomous sensing-healing of delamination in large-scale composite structures. Smart Mater Struct 2014;23:115014. http://dx.doi.org/10.1088/0964-1726/23/11/115014.
[41] ASTM International. ASTM Standard D 638, 2003, "Tensile properties of plastics. West Conshohocken, PA: ASTM International; 2003. http://dx.doi.org/10.1520/D0638-10 [n.d], www.astm.org.
[42] ASTM International. ASTM Stand D 5868, 2001, "Lap shear adhesion for Fiber Reinforced Plastic (FRP)". West Conshohocken, PA: ASTM International; 2003. http://dx.doi.org/10.1520/D5868 [n.d], www.astm.org.
[43] Airbus AITM 1–0019 Determination of lap shear tensile strength of composite joints. In-plane shear by Lap-Shear. Airbus Internal Test Method n.d.
[44] ASTM International. In: ASTM Standard D 5528, 2007, "Mode I interlaminar fracture toughness of unidirectional fiber-reinforced polymer matrix composites", 1. West Conshohocken, PA: ASTM International; 2003. http://dx.doi.org/10.1520/D5528 [n.d], www.astm.org.
[45] ASTM International. ASTM Standard D 3039-14, 2014, "Standard test method for tensile properties of polymer matrix composite materials. Conshohocken, PA: ASTM International; 2003. http://dx.doi.org/10.1520/D3039 [n.d], www.astm.org.
[46] Dow Plastics. Liquid epoxy resins. 1999.
[47] Petrie EM. Epoxy adhesive formulations. 1st ed. McGraw-Hill Professional; 2005.
[48] Pritchard G. Polymer S and T. Plastics additives: an A-Z reference. 1st ed. Chapman & Hall; 1998.
[49] Tong L. Strength of adhesively bonded single-lap and lap-shear joints. Int J Solids Struct 1998;35:2601–16.